

Critical properties of the perovskite manganite $\text{La}_{0.1}\text{Nd}_{0.6}\text{Sr}_{0.3}\text{MnO}_3$

Jiyu Fan,^{1,*} Langsheng Ling,² Bo Hong,³ Lei Zhang,² Li Pi,⁴ and Yuheng Zhang^{2,4}

¹Department of Applied Physics, Nanjing University of Aeronautics and Astronautics, Nanjing 210016, China

²High Magnetic Field Laboratory, Chinese Academy of Sciences, Hefei 230031, China

³Department of Material Engineering, China Jiliang University, Hangzhou 310018, China

⁴Hefei National Laboratory for Physical Sciences at the Microscale, University of Science and Technology of China, Hefei 230026, China

(Received 20 August 2009; revised manuscript received 27 January 2010; published 26 April 2010)

The critical properties of perovskite manganite $\text{La}_{0.1}\text{Nd}_{0.6}\text{Sr}_{0.3}\text{MnO}_3$ around the paramagnetic-ferromagnetic phase transition are investigated through various techniques such as modified Arrott plot, Kouvel-Fisher method, and critical isotherm analysis. The magnetic data analyzed in the critical region using the above methods yield the critical exponents of $\beta=0.257 \pm 0.005$ and $\gamma=1.12 \pm 0.03$ at $T_C=249.32 \pm 0.03$ K. The exponent $\delta=5.17 \pm 0.02$ independently obtained from the critical magnetization isotherm was found to basically fulfill the Widom scaling relation $\delta=1+\gamma/\beta$. Moreover, the critical exponents also obey the single scaling equation of $M(H, \varepsilon)=\varepsilon^\beta f_\pm(H/\varepsilon^{\beta+\gamma})$. These results indicate that the obtained critical exponents are reliable. The values deduced for the critical exponents are closed to the theoretical prediction of tricritical mean-field model rather than the universal theory of three-dimensional Heisenberg model and mean-field model. These results suggest the present composition may be close to a tricritical point in the $\text{La}_{0.7-x}\text{Nd}_x\text{Sr}_{0.3}\text{MnO}_3$ phase diagram.

DOI: [10.1103/PhysRevB.81.144426](https://doi.org/10.1103/PhysRevB.81.144426)

PACS number(s): 75.40.Cx, 75.47.Lx, 64.60.Ht

I. INTRODUCTION

Over the past a few years, the perovskite manganites with ABO_3 -type compounds $RE_{1-x}AE_x\text{MnO}_3$, where RE stands for the trivalent rare-earth element such as La, Pr, Nd, Sm, etc, and AE for the divalent alkaline earth ion such as Sr, Ca Ba, and Pb, have attracted much attention due to their extraordinary magnetic and electronic properties as well as their promise for the potential technological applications.¹⁻³ The perovskite structure generally shows lattice distortion as modifications from the idea cubic structure to orthorhombic or orthorhombic structure mainly due to Jahn-Teller (JT) effect causing the deformation of the MnO_6 octahedron. A prominent feature of these materials is an insulator-metal transition together with a paramagnetic-ferromagnetic (PM-FM) transition giving rise to the well-known colossal magnetoresistance (CMR) effect.^{1,4,5} As for $\text{La}_{1-x}\text{Ca}_x\text{MnO}_3$ ($x \leq 0.3$), CMR effect is associated with the formation of nanoscale polarons that develop at elevated temperatures, truncating the ferromagnetic-metallic state and driving the transition first order.⁶⁻⁸ The basic physics of the ferromagnetic metallic state in the mixed-valent manganites has been extensively understood within the framework of the double-exchange (DE) mechanism and JT effect.⁹⁻¹¹ However, the theory can only partly explain the magnetic properties and electronic transport in this strongly correlated materials because many distinct deviations from the above DE and JT theory have been found in experiments.^{12,13} Up to data, there are no a comprehensive theory to understand the complex phenomena in manganites. Therefore, to understand better the relation between insulator-metal transition and CMR effect, two important questions about PM-FM transition should be clarified: one is the order of phase transition, the other is the common universality class. To make these issues clear, it is necessary to investigate in details the critical exponents at the region of the PM-FM transition.

In the early stage, the critical behavior in the DE model was first described with long-range mean-field theory.^{14,15}

Sequently, dependent on the computational technology for the CMR manganites, Motome and Furulawa^{16,17} suggested that the critical behavior should be attributed to short-range Heisenberg model. Moreover, a few relevant experimental investigations on the critical phenomena also supported this viewpoint due to the obtained value of critical exponents consistently with that in the conventional ferromagnet of Heisenberg model. Based on the study of dc magnetization, Ghosh *et al.*¹⁸ reported that the critical exponent β is equal to 0.37 for the ferromagnet manganite $\text{La}_{0.7}\text{Sr}_{0.3}\text{MnO}_3$. ($\beta=0.365$ in Heisenberg model, the critical exponent β is in contact with the temperature dependence of spontaneous magnetization below the Curie Temperature T_C) A similar critical value of $\beta=0.374$ is also reported in the DE ferromagnet $\text{Nd}_{0.6}\text{Pb}_{0.4}\text{MnO}_3$.¹⁹ However, a relative high value of $\beta=0.5$ obtained in the polycrystalline $\text{La}_{0.8}\text{Sr}_{0.2}\text{MnO}_3$ is in good agreement with that in mean-field model.²⁰ On the contrary, a very low critical exponent of $\beta=0.14$ identified in the single crystal $\text{La}_{0.7}\text{Ca}_{0.3}\text{MnO}_3$ suggested that the PM-FM transition in this system is of first order rather than second order.²¹ Meanwhile, a moderate critical value of $\beta=0.25$ found in the polycrystalline $\text{La}_{0.6}\text{Ca}_{0.4}\text{MnO}_3$ is in excellent agreement with tricritical point values.^{22,23} Therefore, in view of the varied critical exponents β from 0.1 to 0.5, currently, four kinds of different theoretical models, mean-field ($\beta=0.5$), three-dimensional (3D) Heisenberg ($\beta=0.365$), 3D Ising ($\beta=0.325$), and tricritical mean field ($\beta=0.25$), were used to explain the critical properties in manganites. Due to the divergence in these reported critical values, it is worthwhile to study the critical behavior in the analogous perovskite manganites. Here, we present a detailed investigation of the critical phenomena in the manganite $\text{La}_{0.1}\text{Nd}_{0.6}\text{Sr}_{0.3}\text{MnO}_3$.

II. EXPERIMENT

Polycrystalline $\text{La}_{0.1}\text{Nd}_{0.6}\text{Sr}_{0.3}\text{MnO}_3$ sample was prepared by traditional solid-state reaction method. Stoichiometric

quantities of high-purity oxides of the rare earths, SrCO₃, and MnO₂ were thoroughly mixed and ground, then preheated at 1173 K for 24 h. With intermediate grinding, they reacted at 1573 K for 24 h. After pressed into pellets, a final sintering was carried out at 1673 K for 48 h. The structure and phase purity of as-prepared samples were checked by powder x-ray diffraction (XRD) using Cu K α radiation at room temperature. The XRD patterns prove that the structures of all samples are single phase with orthorhombic perovskites structure. Magnetic measurements were performed by using a superconducting quantum interference device magnetometer (Quantum Design MPMS). The magnetic field was applied along the longest semiaxis of the sample to decrease the shape demagnetizing fields as much as possible (this sample's exterior is on the verge of ellipsoid).

III. RESULTS AND DISCUSSION

According to the scaling hypothesis, the critical behavior of a magnetic system showing a second-order magnetic phase transition near the Curie point are characterized by a set of interrelated critical exponents,¹⁴ β (associated with the spontaneous magnetization M_s), γ (associated with the initial magnetic susceptibility χ_0), δ (associated with the critical magnetization isotherm at T_C). As we know, for a first-order ferromagnetic phase transition, the critical exponents are impossibly defined because the applied magnetic field can shift this transition which results in a field dependent phase boundary $T_C(H)$.²³ The mathematical definitions of the critical exponents from magnetization measurements are given as following relation:

$$M_s(T) = M_0 |\varepsilon|^\beta, \quad \varepsilon < 0, \quad T < T_C, \quad (1)$$

$$\chi_0^{-1}(T) = (h_0/M_0) \varepsilon^\gamma, \quad \varepsilon > 0, \quad T > T_C, \quad (2)$$

$$M = DH^{1/\delta}, \quad \varepsilon = 0, \quad T = T_C, \quad (3)$$

where ε is the reduced temperature $(T - T_C)/T_C$, and M_0 , h_0/M_0 , and D are the critical amplitudes.

Generally, the critical exponents and critical temperature can be easily determined from the Arrott plot. According to Arrott-Noakes equation of state, $(H/M)^{1/\gamma} = (T - T_C)/T_C + (M/M_1)^{1/\beta}$,²⁴ where M_1 is a material constant, the regular Arrott plot shows as M^2 vs H/M relationship based on the mean-field model of critical exponent of $\beta=0.5$ and $\gamma=1.0$. Thus, the M^2 vs H/M curves should reveal a linear behavior around T_C and the line at $T=T_C$ should just pass through the origin. Additionally, according to the criterion proposed by Banerjee,²⁵ the order of magnetic transition can be determined from the slope of these straight lines. The positive slope corresponds to the second-order transition while the negative slope corresponds to the first-order transition. Figure 1 shows the Arrott plot M^2 vs H/M for the La_{0.1}Nd_{0.6}Sr_{0.3}MnO₃ sample in the temperature range of $T_C \pm 20$ K. Clearly, in the present case the positive slope of M^2 vs H/M curves indicates the ferromagnetic phase transition to be of the second order. However, all the curves in the Arrott plot are nonlinear and shows upward curvature even at

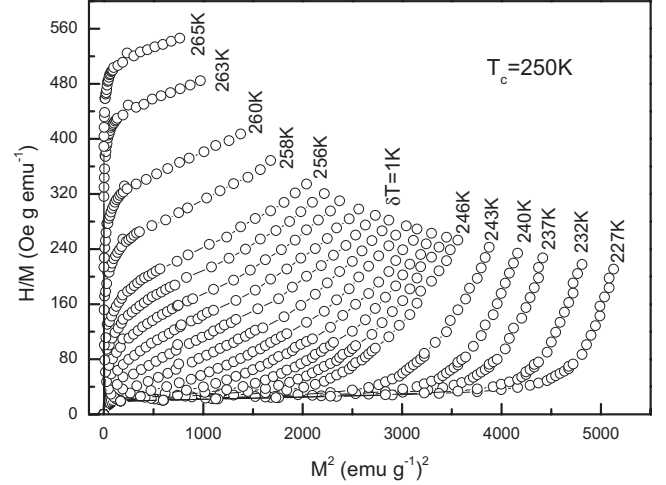


FIG. 1. Arrott plot: isotherms of H/M vs M^2 of La_{0.1}Nd_{0.6}Sr_{0.3}MnO₃ at different temperatures close to the Curie temperature ($T_C=249$ K).

high field indicating the mean-field theory is dissatisfied with the present phase transition. Generally, at high field region, the effect of charge, lattice, and orbital degrees of freedom are suppressed in a ferromagnet and the order parameter can be identified with the macroscopic magnetization. Therefore, to obtain the correct values of β and γ a modified Arrott plot need to yield quasistraight lines of M^2 vs H/M curves. As shown in Figs. 2(a)–2(c), three different kinds of trial exponents of 3D Heisenberg model ($\beta=0.365$, $\gamma=1.336$), 3D Ising ($\beta=0.325$, $\gamma=1.24$), and tricritical mean field ($\beta=0.25$, $\gamma=1.0$), were used to make a modified Arrott plot. For comparing these results, we calculate their relative slopes (RS) which are defined as $RS=S(T)/S(T_C=249$ K). If the modified Arrott plot shows a series of absolute parallel lines, the relative slopes should be kept to 1 irrespective of temperatures. As shown in Fig. 2(d), the RS of Heisenberg and Ising model obviously deviates from the straight line of $RS=1$ but the RS of tricritical mean-field model is close to it. Therefore, the third Arrott plot should be the best results among these three models, indicating the critical properties of La_{0.1}Nd_{0.6}Sr_{0.3}MnO₃ sample can be described with tricritical mean-field model. Thus, in Fig. 2(c), the linear extrapolation from high field region to the intercepts with the axes $H/M^{1/\gamma}$ and $M^{1/\beta}$ yield the reliable values of inverse susceptibility $\chi_0^{-1}(T, 0)$ and spontaneous magnetization $M_s(T, 0)$, respectively. These values as functions of temperatures, $\chi_0^{-1}(T, 0)$ vs T and $M_s(T, 0)$ vs T , are plotted in Fig. 3. According to Eqs. (1) and (2), the experimental data (open sign) can be fitted to two continuous curves (solid line). It gives two new values of $\beta=0.248 \pm 0.006$ with $T_C=249.36 \pm 0.04$ K and $\gamma=1.066 \pm 0.002$ with $T_C=248.90 \pm 0.08$ K. These results are very close to the critical exponent of tricritical mean-field model.

Alternatively, these critical exponents and T_C can be obtained more accurately from the Kouvel-Fisher (KF) method²⁶

$$\frac{M_s(T)}{dM_s(T)/dT} = \frac{T - T_C}{\beta}, \quad (4)$$

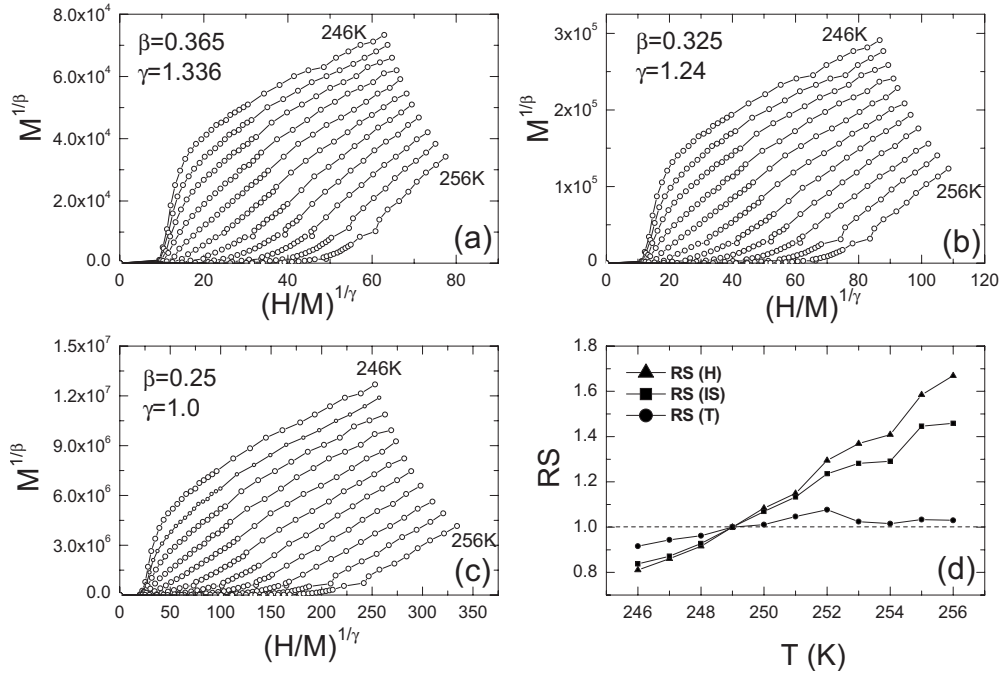


FIG. 2. Modified Arrott plot isotherms of $M^{1/\beta}$ vs $(H/M)^{1/\gamma}$ with: (a) 3D Heisenberg model ($\beta=0.365$, $\gamma=1.336$); (b) 3D Ising model ($\beta=0.325$, $\gamma=1.24$); (c) tricritical mean-field model ($\beta=0.25$, $\gamma=1.0$); and (d) RS vs temperatures: $RS=S(T)/S(T_C=249\text{ K})$, $RS(H) \rightarrow$ Heisenberg model, $RS(IS) \rightarrow$ Ising model, $RS(T) \rightarrow$ Tricritical mean-field model.

$$\frac{\chi_0^{-1}(T)}{d\chi_0^{-1}(T)/dT} = \frac{T - T_C}{\gamma} \quad (5)$$

According to this method, $M_s(dM_s/dT)^{-1}$ vs T and $\chi_0^{-1}(d\chi_0^{-1}/dT)^{-1}$ vs T should yield straight lines with slopes $1/\beta$ and $1/\gamma$, respectively. When these straight lines are extrapolated to the ordinate equal to zero, the intercepts on T axis just correspond to T_C . As presented in Fig. 4, the fitting results with KF method give the exponents and T_C to be of $\beta=0.257 \pm 0.005$ with $T_C=249.32 \pm 0.03$ K and $\gamma = 1.12 \pm 0.03$ with $T_C=249.10 \pm 0.07$ K. Obviously, the obtained values of the critical exponents and T_C using the KF method are in agreement with that using the modified Arrott plot of tricritical mean-field model.

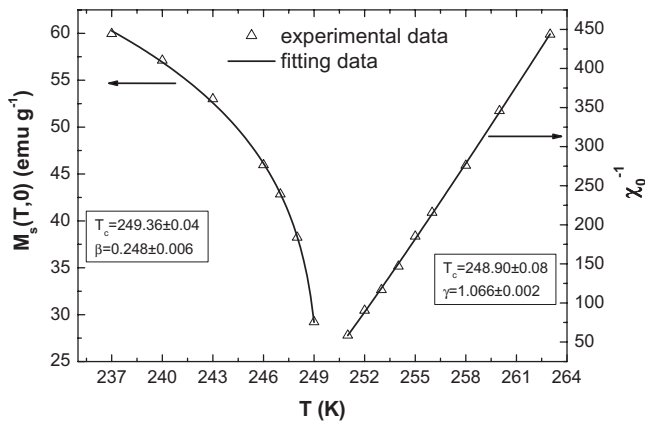


FIG. 3. Temperature as a function of the spontaneous magnetization $M_s(T,0)$ (left, open circles) and the inverse initial susceptibility $\chi_0^{-1}(T)$ (right, open circles) along with the fitting curves based on the power laws (solid lines).

To further check the reliability of the above critical exponents, we can study the relation among the three critical exponents β , γ , and δ . Here, we must know the value of δ first. According to Eq. (3), the value of δ can be directly obtained from plotting the critical isotherm at T_C . In Fig. 5, the M vs H curve at 249 K was chosen as the critical isotherm based on the previous discussion. The inset of Fig. 5 shows the same curve M vs H on a log-log scale. The solid straight line with a slope $1/\delta$ is the fitting result by using Eq. (3). From the linear fit we obtained the third critical exponent $\delta = 5.17 \pm 0.02$. According to statistical theory, these three critical exponents must fulfill the Widom scaling relation

$$\delta = 1 + \frac{\gamma}{\beta} \quad (6)$$

Based on the above obtained data of β and γ , Eq. (6) yields the value of $\delta=5.298$ for β and γ evaluated from Fig.

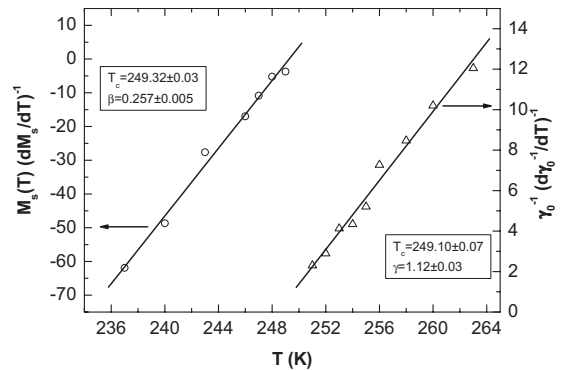


FIG. 4. Kouvel-Fisher plots for the spontaneous magnetization M_s (left) and the inverse initial susceptibility χ_0^{-1} (right).

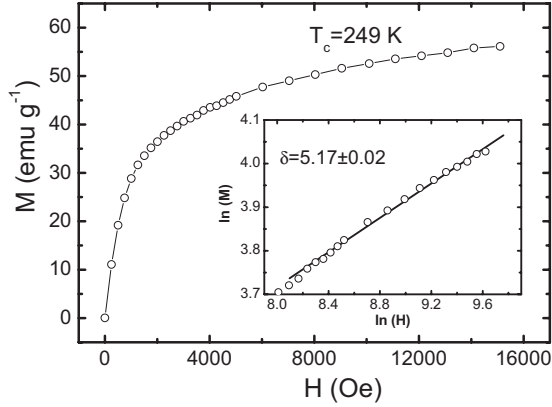


FIG. 5. Isothermal M vs H plot of $\text{La}_{0.1}\text{Nd}_{0.6}\text{Sr}_{0.3}\text{MnO}_3$ at $T_C = 249$ K; the inset shows the same plot in log-log scale and the solid line is the linear fit following Eq. (3).

3 and $\delta = 5.358$ for β and γ obtained from Fig. 4. Both of the critical exponents δ approximate to the estimated δ from the critical isotherms at T_C . Therefore, the critical exponents obtained in this study basically obey the Widom scaling relation, implying that the obtained β and γ data are reliable.

In the critical region, the magnetic equation can be written as

$$M(H, \varepsilon) = \varepsilon^\beta f_\pm(H/\varepsilon^{\beta+\gamma}), \quad (7)$$

where f_+ for $T > T_C$ and f_- for $T < T_C$ are regular functions.²⁷ Eq. (7) indicates that $M\varepsilon^{-\beta}$ as a function of $H\varepsilon^{-(\beta+\gamma)}$ yields two universal curves: one for temperature $T > T_C$ and the other for temperature $T < T_C$. Thus we can compare the obtained results with the prediction of the scaling theory with Eq. (7). As shown in the Fig. 6, the experimental data fall on two curves, one above T_C and the other below T_C , in agreement with the scaling theory. The inset of Fig. 6 shows the same plot on log-log scale. Similarly, all the points also collapse into two different curves. This result further indicates that the obtained values of the critical exponents and T_C are reliable. Moreover, the characterization of the critical prop-

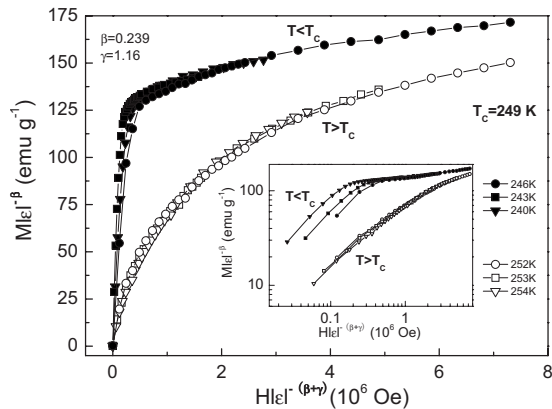


FIG. 6. Scaling plots below and above T_C using β and γ determined from Kouvel-Fisher method; the inset shows the same plot in log-log scale.

erties with the tricritical mean-field model is accurate in the present system.

At present, the 3D Heisenberg model is extensively used to discuss critical properties and understand the short-range interaction in the doping manganites. Nevertheless, some experimental results indicate that other theoretical models, such as mean-field and tricritical mean-field model, are better to describe the critical behavior in manganites. Here, some critical exponents reported in the manganites are summarized in Table I. From it, one can find that the obtained critical exponents β mainly center a range of 0.3–0.4, similar to those of 3D Heisenberg ferromagnet that has critical indices $\beta = 0.368$.³⁴ Nevertheless, the reported value of γ in the Table I is not close to the theoretical index of 3D Heisenberg model.¹⁵ Moreover, the $\text{La}_{0.7}\text{Ca}_{0.3}\text{MnO}_3$ single crystal shows a first-order transition.²¹ Therefore, a crossover to a continuous phase transition should occur in manganites. Generally, the critical exponents of ferromagnetic phase transition are determined by the type of ordering and the dimensionality.³⁵ However, at a tricritical point, Huang²² proposed that these critical exponents should be universal. Kim *et al.*²³ reported the tricritical point in the polycrystal $\text{La}_{0.6}\text{Ca}_{0.4}\text{MnO}_3$, in agreement with theoretical prediction. This tricritical point separates first-order ($x < 0.4$) from second-order ($x > 0.4$) phase transition. In the present system, as shown in Fig. 2(c), the obtained critical indices are consistent with that in tricritical mean-field model. It suggests that the present composition may be close to a tricritical point in the $\text{La}_{0.7-x}\text{Nd}_x\text{Sr}_{0.3}\text{MnO}_3$ phase diagram. As we know, the properties of manganites are strongly affected by chemical factor of average cationic radius $\langle r_A \rangle$ in A site.^{36,37} The decrease in $\langle r_A \rangle$ tends to diminish the Mn-O-Mn angle and reduce the bandwidth and T_C . According to Ref. 38, the decreases of the Mn-O-Mn angle and the bandwidth weaken the hopping integral of e_g electrons, and consequently attenuate the double exchange interaction between Mn^{3+} and Mn^{4+} ions. Comparing with $\text{Nd}_{0.7}\text{Sr}_{0.3}\text{MnO}_3$, the average cationic radius $\langle r_A \rangle$ of $\text{La}_{0.1}\text{Nd}_{0.6}\text{Sr}_{0.3}\text{MnO}_3$ is slightly increased due to $r_{\text{La}} > r_{\text{Nd}}$. Therefore, the higher T_C and stronger ferromagnetism was observed in the latter. Recently, the first-order FM-PM transition was reported in the manganite $\text{Nd}_{0.7}\text{Sr}_{0.3}\text{MnO}_3$ at $T_C = 207$ K.³⁹ Nevertheless, a second-order phase transition was testified in the $\text{Nd}_{0.6}\text{Sr}_{0.4}\text{MnO}_3$ at $T_C = 272$ K.⁴⁰ Here, both of their average radius of $\langle r_A \rangle$ are calculated to be $\langle r_A \rangle = 1.2071$ Å and $\langle r_A \rangle = 1.2218$ Å using nine-coordinated ionic radii given by Shannon,⁴¹ respectively. The average radius of the present sample $\text{La}_{0.1}\text{Nd}_{0.6}\text{Sr}_{0.3}\text{MnO}_3$ is $\langle r_A \rangle = 1.2124$ Å, which just locates in the center of the above range. Therefore, a tricritical point is possible to occur in the present materials. Interestingly, a possible tricritical point was recently pointed out in $\text{Nd}_{0.67}\text{Sr}_{0.33}\text{MnO}_3$ with $\langle r_A \rangle = 1.2115$ Å.⁴⁰ Both of their average radius $\langle r_A \rangle$ are quite similar. On the other hand, the recent investigations indicate that the doping manganites are intrinsic inhomogeneity with multiphase coexistence and phase competition which induce the complexity in this system.^{12,13,42} Regarding the magnetic properties in $\text{Nd}_{0.7}\text{Sr}_{0.3}\text{MnO}_3$, the competition between the double exchange ferromagnetic interaction and the superexchange antiferromagnetic interaction was earlier found even in the metallic ferromagnetic phase.⁴³ In our

TABLE I. Critical parameters of $\text{La}_{0.1}\text{Nd}_{0.6}\text{Sr}_{0.3}\text{MnO}_3$ with theoretical models and other manganites reported in literature. Abbreviations: PC, polycrystalline; SC, single crystal.

Composition	Ref.	T_C (K)	β	γ	δ
$\text{La}_{0.1}\text{Nd}_{0.6}\text{Sr}_{0.3}\text{MnO}_3$ (PC)	This work	249	0.249	1.16	5.17
Tricritical mean-field theory	22		0.25	1.0	5.0
Mean-field theory	27		0.5	1.0	3.0
3D Heisenberg theory	27		0.365	1.336	4.8
3D Ising theory	27		0.325	1.24	4.82
$\text{La}_{0.8}\text{Ca}_{0.2}\text{MnO}_3$ (SC)	28		0.36	1.45	
$\text{La}_{0.7}\text{Ca}_{0.3}\text{MnO}_3$ (SC)	21	222	0.14	0.81	1.22
$\text{La}_{0.6}\text{Ca}_{0.4}\text{MnO}_3$ (PC)	23	265.5	0.25	1.03	5.0
$\text{La}_{0.8}\text{Sr}_{0.2}\text{MnO}_3$ (PC)	20	315.74	0.5	1.08	3.13
$\text{La}_{0.7}\text{Sr}_{0.3}\text{MnO}_3$ (SC)	18	354	0.37	1.22	4.25
$\text{La}_{0.875}\text{Sr}_{0.125}\text{MnO}_3$ (SC)	29	186	0.37	1.38	4.72
$\text{La}_{0.67}\text{Ba}_{0.33}\text{MnO}_3$ (PC)	30	306	0.356	1.12	
$\text{Nd}_{0.6}\text{Pb}_{0.4}\text{MnO}_3$ (SC)	19	156.47	0.374	1.329	4.54
$\text{Sm}_{0.52}\text{Sr}_{0.48}\text{MnO}_3$ (SC)	31	110	0.32	1.31	
$\text{Pr}_{0.77}\text{Ca}_{0.23}\text{MnO}_3$ (SC)	32	167.08	0.344	1.352	4.66
$\text{Pr}_{0.70}\text{Ca}_{0.30}\text{MnO}_3$ (SC)	32	197.58	0.404	1.357	4.52
$\text{Pr}_{0.50}\text{Sr}_{0.50}\text{MnO}_3$ (PC)	33	261.4	0.448	1.334	3.977

sample, the increase in average cationic radius $\langle r_A \rangle$ facilitates ferromagnetic interaction and induces stronger competition in the system. As a result, the rise of spin-orbit coupling can transfer the discontinuous phase transition to continuous phase transition. Thus, a tricritical point was observed in the $\text{La}_{0.1}\text{Nd}_{0.6}\text{Sr}_{0.3}\text{MnO}_3$ sample. This finding should provide a point of reference for an understanding of the anomalous PM-FM transition in manganites. Up to now, although the wide disparity of critical phenomena have been reported in the literature, it is difficult to determine the common universality class for a continuous PM-FM phase transitions in manganites. The better method for this issue need more experimental measurements on high purity samples with different compositions.

IV. CONCLUSION

In summary, the critical properties of the perovskite manganite $\text{La}_{0.1}\text{Nd}_{0.6}\text{Sr}_{0.3}\text{MnO}_3$ have been studied using the iso-

thermal magnetization around Curie point T_C . Based on various research techniques including modified Arrott plot, Kouvel-Fisher method, and critical isotherm analysis, the obtained critical exponents of β and γ are in agreement to the theoretical value of tricritical mean-field model. This result implies that the present composition might be close to the tricritical point in the $\text{La}_{0.7-x}\text{Nd}_x\text{Sr}_{0.3}\text{MnO}_3$ phase diagram. Even though the 3D Heisenberg model was extensively used to describe the critical behavior in manganite, the strong discrepancy of the reported critical indices indicates that further investigation on this issue is necessary.

ACKNOWLEDGMENTS

This work was supported by the young research funding of Nanjing University of Aeronautics and Astronautics and the National Nature Science Foundation of China (Grants No. 10334090 and No. 10504029).

*fanjiyu@gmail.com

¹S. Jin, T. H. Tiefel, M. McCormack, R. A. Fastnacht, R. Ramesh, and L. H. Chen, *Science* **264**, 413 (1994).

²A. Moreo, S. Yunoki, and E. Dagotto, *Science* **283**, 2034 (1999).

³M. B. Salamon and M. Jaime, *Rev. Mod. Phys.* **73**, 583 (2001).

⁴E. Dagotto, T. Hotta, and A. Moreo, *Phys. Rep.* **344**, 1 (2001).

⁵M. Fäth, S. Freisem, A. A. Menovsky, Y. Tomioka, J. Aarts, and J. A. Mydosh, *Science* **285**, 1540 (1999).

⁶J. W. Lynn, R. W. Erwin, J. A. Borchers, Q. Huang, A. Santoro, J.-L. Peng, and Z. Y. Li, *Phys. Rev. Lett.* **76**, 4046 (1996).

⁷P. Dai, J. A. Fernandez-Baca, N. Wakabayashi, E. W. Plummer, Y. Tomioka, and Y. Tokura, *Phys. Rev. Lett.* **85**, 2553 (2000).

⁸J. A. Fernandez-Baca, P. Dai, H. Y. Hwang, C. Kloc, and S.-W. Cheong, *Phys. Rev. Lett.* **80**, 4012 (1998).

⁹C. Zener, *Phys. Rev.* **82**, 403 (1951).

¹⁰A. J. Millis, P. B. Littlewood, and B. I. Shraiman, *Phys. Rev. Lett.* **74**, 5144 (1995).

¹¹A. J. Millis, *Phys. Rev. B* **53**, 8434 (1996).

¹²M. Uehara, S. Mori, C. H. Chen, and S.-W. Cheong, *Nature (London)* **399**, 560 (1999).

- ¹³J. M. De Teresa, M. R. Ibarra, P. A. Algarabel, C. Ritter, C. Marquina, J. Blasco, J. Garcia, A. del Moral, and Z. Arnold, *Nature (London)* **386**, 256 (1997).
- ¹⁴H. E. Stanley, *Introduction to Phase Transitions and Critical Phenomena* (Oxford University Press, London, 1971).
- ¹⁵M. Seeger, S. N. Kaul, H. Kronmüller, and R. Reisser, *Phys. Rev. B* **51**, 12585 (1995).
- ¹⁶Y. Motome and N. Furulawa, *J. Phys. Soc. Jpn.* **69**, 3785 (2000).
- ¹⁷Y. Motome and N. Furulawa, *J. Phys. Soc. Jpn.* **70**, 1487 (2001).
- ¹⁸K. Ghosh, C. J. Lobb, R. L. Greene, S. G. Karabashev, D. A. Shulyatev, A. A. Arsenov, and Y. Mukovskii, *Phys. Rev. Lett.* **81**, 4740 (1998).
- ¹⁹J. Hafner and D. Hobbs, *Phys. Rev. B* **68**, 014408 (2003).
- ²⁰Ch. V. Mohan, M. Seeger, H. Kronmüller, P. Murugaraj, and J. Maier, *J. Magn. Magn. Mater.* **183**, 348 (1998).
- ²¹H. S. Shin, J. E. Lee, Y. S. Nam, H. L. Ju, and C. W. Park, *Solid State Commun.* **118**, 377 (2001).
- ²²K. Huang, *Statistical Mechanics*, 2nd ed. (Wiley, New York, 1987).
- ²³D. Kim, B. Revaz, B. L. Zink, F. Hellman, J. J. Rhyne, and J. F. Mitchell, *Phys. Rev. Lett.* **89**, 227202 (2002).
- ²⁴A. Arrott and J. E. Noakes, *Phys. Rev. Lett.* **19**, 786 (1967).
- ²⁵B. K. Banerjee, *Phys. Lett.* **12**, 16 (1964).
- ²⁶J. S. Kouvel and M. E. Fisher, *Phys. Rev.* **136**, A1626 (1964).
- ²⁷S. N. Kaul, *J. Magn. Magn. Mater.* **53**, 5 (1985).
- ²⁸C. S. Hong, W. S. Kim, and N. H. Hur, *Phys. Rev. B* **63**, 092504 (2001).
- ²⁹S. Nair, A. Banerjee, A. V. Narlikar, D. Prabhakaran, and A. T. Boothroyd, *Phys. Rev. B* **68**, 132404 (2003).
- ³⁰N. Moutis, I. Panagiotopoulos, M. Pissas, and D. Niarchos, *Phys. Rev. B* **59**, 1129 (1999).
- ³¹P. Sarkar, P. Mandal, A. K. Bera, S. M. Yusuf, L. S. Sharath Chandra, and V. Ganesan, *Phys. Rev. B* **78**, 012415 (2008).
- ³²B. Padmanabhan, H. L. Bhat, S. Elizabeth, S. Rössler, U. K. Rössler, K. Dörr, and K. H. Müller, *Phys. Rev. B* **75**, 024419 (2007).
- ³³A. K. Pramanik and A. Banerjee, *Phys. Rev. B* **79**, 214426 (2009).
- ³⁴M. Campostrini, M. Hasenbusch, A. Pelissetto, P. Rossi, and E. Vicari, *Phys. Rev. B* **65**, 144520 (2002).
- ³⁵M. E. Fisher, S. K. Ma, and B. G. Nickel, *Phys. Rev. Lett.* **29**, 917 (1972).
- ³⁶H. Y. Hwang, S. W. Cheong, P. G. Radaelli, M. Marezio, and B. Batlogg, *Phys. Rev. Lett.* **75**, 914 (1995).
- ³⁷A. Maignan, Ch. Simon, V. Caignaert, and B. Raveau, *Solid State Commun.* **96**, 623 (1995).
- ³⁸P. G. Radaelli, G. Iannone, M. Marezio, H. Y. Hwang, S.-W. Cheong, J. D. Jorgensen, and D. N. Argyriou, *Phys. Rev. B* **56**, 8265 (1997).
- ³⁹R. Venkatesh, M. Patabiraman, S. Angappane, G. Rangarajan, K. Sethupathi, J. Karatha, M. Fecioru-Morariu, R. M. Ghadimi, and G. Guntherodt, *Phys. Rev. B* **75**, 224415 (2007).
- ⁴⁰R. Venkatesh, M. Patabiraman, K. Sethupathi, G. Rangarajan, S. Angappane, and J.-G. Park, *J. Appl. Phys.* **103**, 07B319 (2008).
- ⁴¹R. D. Shannon, *Acta Crystallogr., Sect. A: Cryst. Phys., Diffraction, Theor. Gen. Crystallogr.* **32**, 751 (1976).
- ⁴²J. Burgy, M. Mayr, V. Martin-Mayor, A. Moreo, and E. Dagotto, *Phys. Rev. Lett.* **87**, 277202 (2001).
- ⁴³J.-G. Park, M. S. Kim, H.-C. Ri, K. H. Kim, T. W. Noh, and S.-W. Cheong, *Phys. Rev. B* **60**, 14804 (1999).